Near-Ultrasonic Time-Reversal Indoor Communication

Arthur Aubertin[1,2,3], Pierre Jouvelot[2], Julien De Rosny[3]

[1]Stimshop, 3bis rue Taylor, Paris, France

[2]MINES ParisTech, Université PSL, Paris, France

[3]ESPCI Paris, Université PSL, Paris, France

May 4, 2021

Abstract

For some indoor applications, the use of radio-frequency telecommunication means is not deemed suitable. As an efficient alternative, we present a new acoustic airborne communication system, based on near-ultrasound, chirp modulation and time-reversal mirroring. Using near ultrasound minimizes users' hearing discomfort while nevertheless remaining compatible with standard audible acoustic devices. To take advantage of spatial diversity, the system relies upon a base station consisting of a 8-channel time-reversal mirror (TRM). Communication is then performed between this TRM and 2 dedicated acoustic transceivers developed for this study. Data transfer performance is assessed in very diverse indoor environments and with different ranges. TRM brings a clear improvement in some key configurations. An exciting application field for near-ultrasonic wireless communication is smartphones; we thus tested our system performances with such a device. Because the loudspeaker and microphone on smartphones are usually not located at the same position, the system focusing quality strongly depends on the method used to acquire the channel responses between the smartphone and the TRM.

1 Introduction

Acoustics-based communication can be a relevant alternative to radio-based communication, for instance in ATEX[1] restricted areas, in environments where strong electromagnetic interference is experienced or when a high level of security is required. Consequently, many companies have expressed, for several years, a renewed interest in the use of audible and ultrasonic airborne communication. One motivation for this is the simplicity of setting up such a technology on various systems such as Public Address (PA) systems, smartphones, computers and many IoT (Internet Of Things) systems equipped with a microphone and/or loudspeaker.

To improve communication efficiency, several methods initially developed for radio communications have been transposed to acoustics. For instance, an ultrasonic transmission of 0.8 Mb/s has been reached using Quadratic Amplitude Modulation (QAM) combined to Orthogonal Frequency Division Multiplexing (OFDM) [JW16]. However, such a high data rate is only obtained when the emitter and receiver are 1.5 m apart. The communication throughput collapses to 100 kb/s at a 20-meter distance, since, for large distances, the signal-to-noise ratio dramatically decreases. In such cases, a modulation based on chirp compression, i.e., spectral spreading, can be used (see, e.g., [Wan15]). This technique has been transposed to near ultrasound at 20 kHz [LR12] to simultaneously transmit data and localized users.

Smartphones represent today an ubiquitous element in telecommunications and embed many RF communication systems (BLE, 4G, NFC, etc.). However, only a few works are dedicated to acoustic communications

[1]"Atmosphère explosive" (in French), or explosive atmosphere.

with such devices. In order to use the built-in microphone and loudspeaker but without disturbing the user, studies focus on the near-ultrasound spectrum that lies between 15 kHz and 20 kHz. For instance, an error-free communication up to 0.8 m with an encoding based on the variation of symbol time has be achieved [AB11]. Considering more complex encodings, such as direct-sequence spread spectrum, P. Getreuer et al. [Get+18] have worked on almost-error-free smartphone-to-smartphone communications with a range of 2 m and a bit rate of 94 bit/s.

In all these studies, the throughput is intrinsically limited because of the SISO (Single Input Single Output) configuration used, where only a single loudspeaker transmits the data. However, the use of arrays of emitters can help alleviate this limit. Of course, in such a MIMO (Multiple Input Multiple Output) configuration, more computer processing is required. Conventional beamforming is one of the simplest methods to focus data on a particular user. However this solution is only valid for outdoor environments. Indeed, for indoor ones, such as in closed rooms, the time shifts introduced by beamforming can only account for the line-of-sight (LoS) contributions but not for the reverberated ones. To overcome this limitation, one can advantageously use a Time-Reversal Mirror (TRM). This technique, based on the time reversal invariance of audio wave propagation, has been first introduced during the 90's to focus ultrasonic waves in water through an aberating media [Fin92; FWT92; CF92]. Later, it has been shown that TRMs are still efficient in complex media such as rod forests or chaotic cavities [DRF95; DF97]. The application of this adaptative focusing technique has been studied in many different fields: non-destructive testing [CFW95], hyperthermia [TF96], shock-wave generation [TWF96], imaging [WRC04] ...

Wireless communications also became a major research area for TRM technology after the success of underwater data transfer between two ships using a TRM [Ede+02; Son16]. While reflections scramble classical wireless communications, ultrasonic scale experiments have shown that TRM takes advantage of such multipaths even in very strong multiple-scattering media [Der+03]. In 2004, the concept of TRM has also been validated for electromagnetic waves [Ler+04; SKC04]. Shortly after, ultra-wideband radio communications based on TRM have been studied [Ler+05; ZGQ06], and it has been observed that TRM usage hardens the channel [El-+10]. Besides these single-carrier modulation experiments, some works were devoted to more complex modulations such as Orthogonal Frequency Division Multiplexing (OFDM) [Dub+13; Dub+14]. More recently, a renewal of interest for solutions involving TRM occurred due to the introduction of the fifth generation of mobile networks and the development of massive MIMO systems. Indeed, the use of large TRMs in such a setting appears as an almost optimal solution [Kon+15; BLM16], especially for mm-wave applications [VTS15]. TRM is also a relevant solution for low-energy radio transmissions dedicated to Internet of Things (IoT).

To the best of our knowledge, the number of studies related to aeroacoustic wireless communications involving TRMs is limited. In 2003, a demonstration of binary data transmission with a data rate of 2.5 kbits/s has been performed through a wall separating 2 rooms. The loudspeaker array was composed of 16 elements and the carrier frequency (main frequency components) was equal to 2.5 kHz [YTF03]. Soon after, TRM-based transmissions at 1 kHz were tested inside a stairway that acted as a highly reverberant environment between one [Can+04] or several loudspeakers [Can+05] and a microphone.

In our work, we propose to address more realistic configurations to test the ability of TRMs to efficiently transmit data. First, we suggest to use a compact TRM composed of 8 elements distributed over a length of 40 cm. This TRM is more than twice shorter that the ones used in [YTF03; Can+04; Can+05]. Second, instead of transmitting data in the middle of the audible frequency range, we choose the near-ultrasonic band (between 17 kHz and 25 kHz). This frequency interval, seldom studied for communication purposes, enables the use of a wide choice of devices developed for general-public applications, while limiting hearing discomfort. Third, instead of using a conventional modulation (BPSK or QPSK), the data is transmitted using a time-domain encoding based on "chirps". Combined with a TRM, this approach ensures a strong detection robustness against ambient noise and interferences. Fourth, a wide variety of tests have been performed inside buildings in various realistic configurations. Finally, data-transmission quality between the TRM and one and/or 2 "users" is evaluated. A user is here equipped with either a dedicated transceiver or a smartphone. The main conclusion of this paper is that, for most of the configurations tested, the use of TRM-based communication significantly improves transmission performance. Nevertheless, the use of smartphones induces some limitations, which are discussed in the sequel.

The structure of the article is the following. In Section 2, the concepts of a near-ultrasound TRM is introduced. The experimental setup and details about channel estimation are presented in Section 3.1. Then the communication performance between a TRM and two dedicated transceivers is studied in a realistic indoor environment for LoS (Line-of-Sight) and NLoS (Non-Line-of-Sight) configurations, in Section 4. Section 5 deals with the use of a smartphone as "user" inside two different environments: first, we analyze the impact of the non-colocalization of the microphone and loudspeaker on TRM focusing; then, communication efficiency is evaluated. We discuss our the results in Section 6, and, finally, Section 7 concludes the paper.

2 Telecommunication by TRM

A Time Reversal (TR) process involves two steps [CWF90]. During the first step, the so-called "learning step", the field emitted by a user (the term "user" is commonly adopted in communication theory to denote one end of a communication channel) is recorded at many points of a control surface. During the second step, the so-called "focusing step", the recorded fields are flipped in time and sent back from each of the aforementioned points. Thanks to the time reversal invariance of propagation, the TR field focuses back at the user location. A perfect focusing can be expected if the control surface forms a close cavity around the user and the field is sampled every half of the smallest wavelength, to fulfill the Shannon-Nyquist theorem. However, such an implementation would be titanic. Nevertheless, M. Fink et al. [PWF91] have shown that a Time-Reversal Mirror (TRM) composed of a limited number of transceivers was in fact sufficient to obtain a good focusing [Fin97; CWF90] on one or several positions.

Figure 1 illustrates the two steps of TR between a user and a TRM. The signal focused by a TRM can be derived from the theory of linear systems. Let's consider a set of K users and a TRM made of M transceivers. During the learning step, signals $e_k(t)$ are emitted by K users ($k \in [1, K]$). The field recorded by each element m of the TRM can be written in terms of convolutions of channel impulse responses (CIR):

$$s_m(t) = \sum_{k=1}^{K} h_{km}(t) * e_k(t), \tag{1}$$

where $h_{km}(t)$ is the CIR between the k-th user and the m-th element of the TRM. The recorded signals are then flipped in time, i.e., $s_m(t)$ gets replaced by $s_m(-t)$, and sent back by each element of the TRM. As a consequence, the expression of the signal $z_{k'}(t)$ received by the user k' is

$$z_{k'}(t) = \sum_{m=1,k=1}^{M,K} h_{mk'}(t) * h_{km}(-t) * e_k(-t). \tag{2}$$

In a reciprocal medium, $h_{km}(t) = h_{mk}(t)$, and therefore the focusing is driven by the correlation of the CIRs $\sum_{m=1}^{M} h_{k'm}(t) * h_{km}(-t)$. In an ideal focusing configuration, this term would be proportional to $\delta_{k,k'}\delta(t)$, i.e., all the TR field focused at time $t = 0$ and at the targeted user position k. In such a case, the focused signal is therefore proportional to $e_k(-t)$.

To take advantage of the focusing property to transmit data, one has to adapt the TR process. The first step consists now of sounding the channels, i.e., to acquire the $K \times M$ CIR $h_{km}(t)$ (within the working frequency bandwidth). This can be done by emitting a chirp. The deconvolution of the known chirp to the response leads to the impulse response. In the second step, the signal $e_k(t)$ to transmit to the k-th user the binary data is worked out from a collection of Γ symbols $S_\gamma(t)$. It is given by

$$e_k(t) = \sum_{l=1,\gamma=\Sigma(l),}^{L} S_\gamma(t - l\tau). \tag{3}$$

where τ is the time interval between emitted symbols and $\Sigma(l)$, for $l \in [1, L]$, is the symbol sequence unequivocally related to the bits to transmit. Before being emitted by the m-th element of the TRM, this signal is convoluted by $h_{km}(-t)$. Finally, the signal received by the k'-th user, is written

$$z_{k'}(t) = \sum_{m=1,k=1}^{M,K} h_{mk'}(t) * h_{km}(-t) * e_k(t) + w_{k'}(t). \tag{4}$$

This expression is very similar to Equation 2, but now the modulated signal $e_k(t)$ is focused, and the contribution of the noise is taken into account by the mean of $w_{k'}(t)$. For simplicity, $w_{k'}(t)$ is assumed to be white, additive and Gaussian.

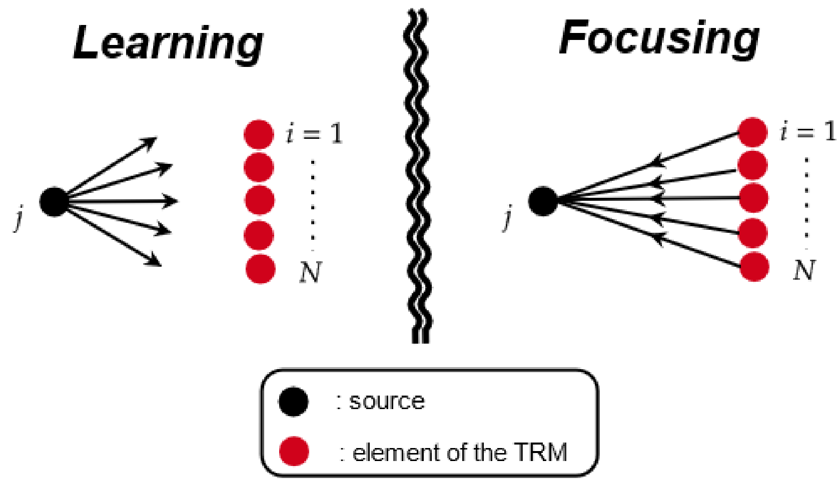

Figure 1: Learning and focusing steps of TR focusing between a source j and a TRM of N transceivers.

Because of the limited aperture of a TRM, the focusing is not perfect. This fact has two consequences: inter-symbol interferences (ISI) and inter-user interferences (IUI). IUI results from imperfect spatial focusing: a symbol focused on one user will perturb the reception of another user. But, even with only a single user, the symbol decoding can be scrambled by some echoes or secondary lobes reaching the user at $t \neq 0$, leading to symbol overlapping (ISI). Another source of possible focusing reduction is the actual lack of reciprocity. It can be due to the presence of an air flow (medium reciprocity) or, more simply, because the source and the receiver are not reciprocal from each other.

3 Time-Reversal Mirror System

The TRM system we set up for our experiments is described and characterized.

3.1 Setup

A mono-element (ME) is the assembly of a Dayton Audio ND16FA-6 speaker (33 mm in diameter, max 10 W emission power) and an electret microphone (4 mm in diameter), both mounted in a 3D-printed case. The microphone is placed as close as possible in front of the center of the loudspeaker via a nylon thread.

The MEs alone, as well as the antenna, described below, were characterized inside an anechoic chamber at Sorbonne University (Paris, France). The directivity diagrams of the MEs show a wide aperture at -3 dB of about 45 degrees in emission and 30 degrees in reception. The loudspeaker and the microphone are connected to a 3 W power amplifier and a pre-amplifier including a phantom power, respectively. Putting together 8 of those MEs allows us to build a 40 cm-wide TRM (see Figure 3.1). The MEs are connected to a 32-channel and 24-bit-AD/DA sound card (Orion 32). The soundcard is connected to a PC laptop running Windows by a USB connection, and controlled by python scripts via an ASIO driver. The audio signals are sampled at a rate of 48 kS/s. .

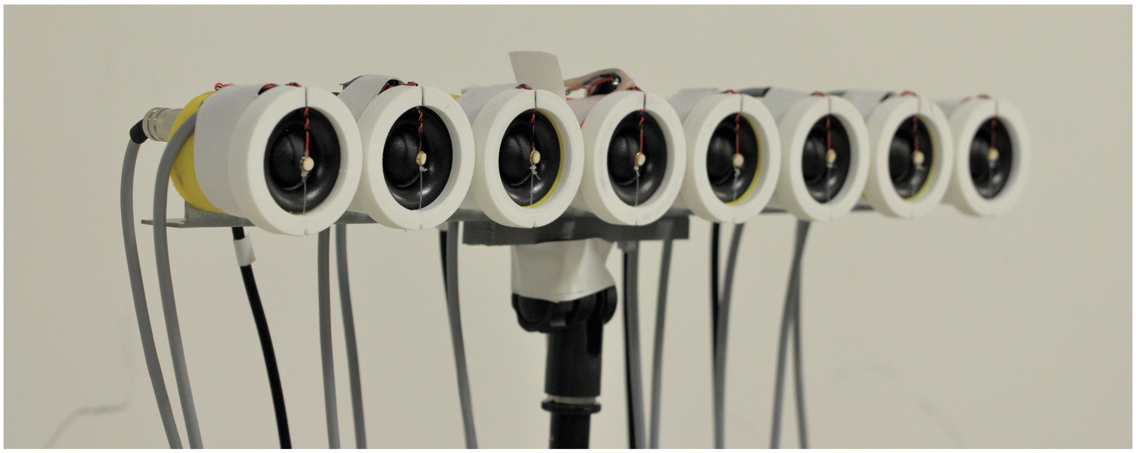

Figure 2: Experimental TRM, made of 8 MEs.

For this work, we consider two different experimental setups in which we test our TRM. In the first one, called setup A, our TRM focuses simultaneously on two independent MEs also connected to the 32-channel sound card. In the second one, called setup B, the TRM targets a smartphone. To handle that latter case, we developed a low-level Android application to control the smartphone loudspeaker and 2 microphones via a Wi-Fi connection. The acquisition chains, corresponding to those setups, are represented in Figure 3.

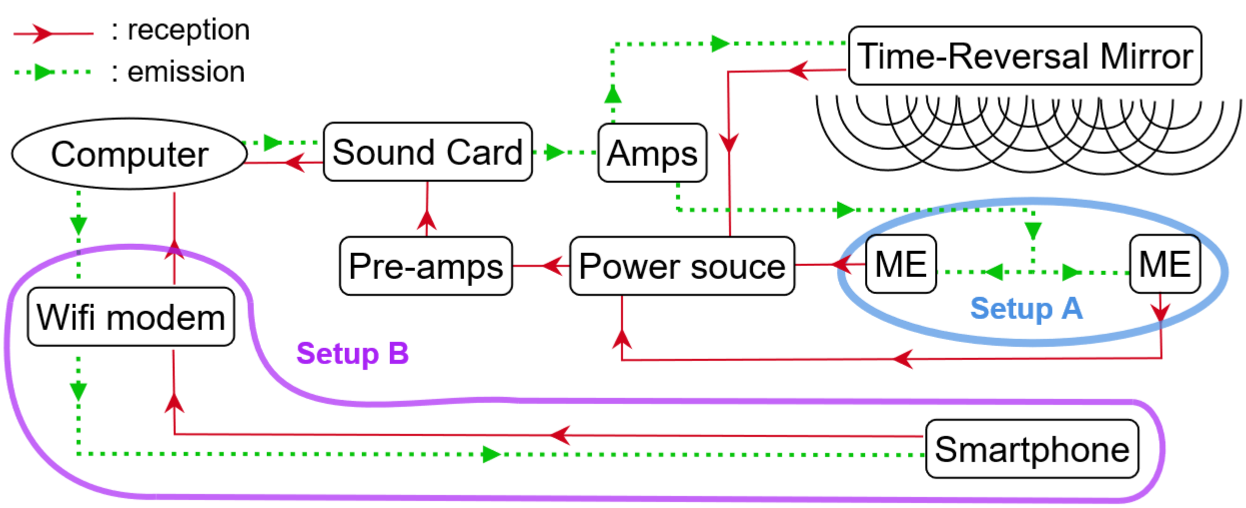

Figure 3: Acquisition chains for the setups A and B.

3.2 Channel Estimation

There are two methods to assess the CIR between the TRM elements and a user. Each of them has its own advantages and disadvantages. They are illustrated in Figure 4, when the user is a smartphone.

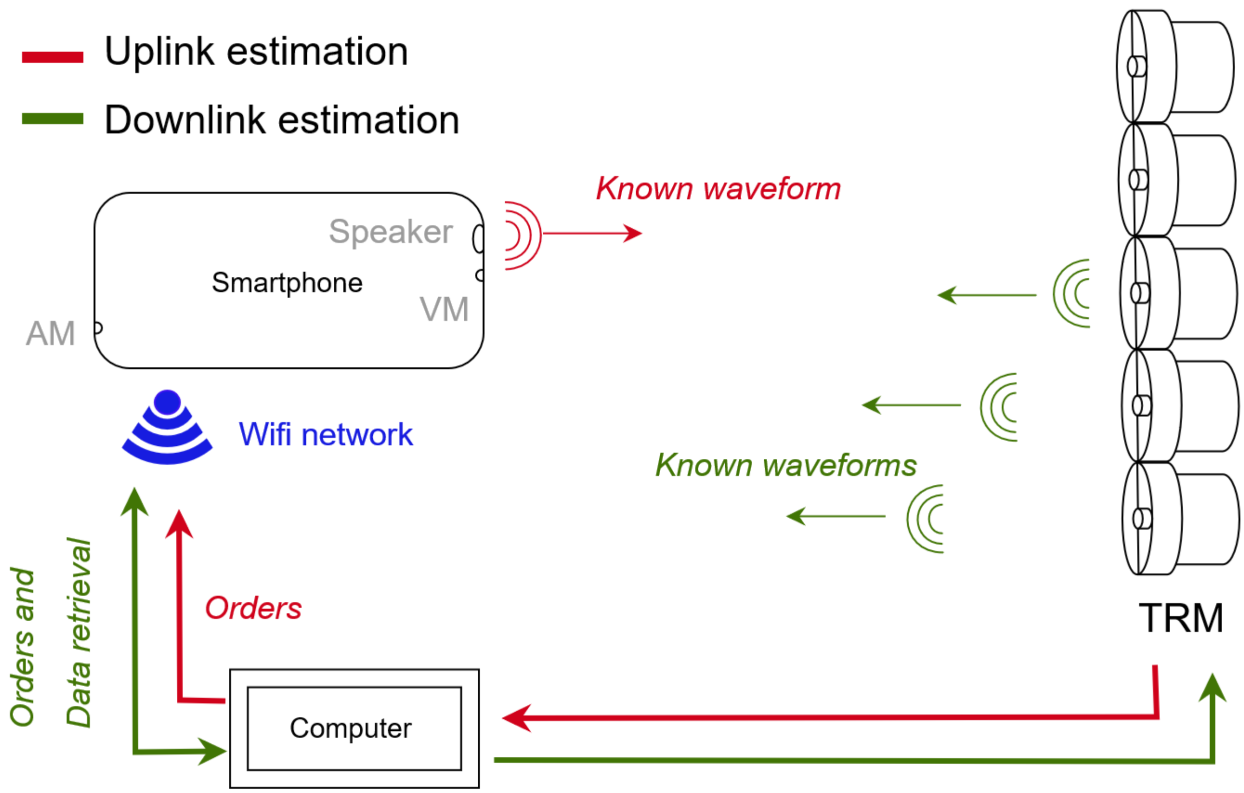

Figure 4: Bidirectional and unidirectional estimations of the propagation channel between a smartphone and a TRM.

For the first approach, called "uplink estimation", the CIRs are computed between the user and the TRM by having the user send signals to the TRM for channel assessment. As explained previously, to focus in an efficient manner, the impulse responses should be reciprocal. This condition is rather well fulfilled when the user consists of a ME, but we are going to see that it is only partially valid in case of a smartphone, because of the non-colocalization of the speaker and microphones .

A more robust approach relies on the measurement of the CIRs between the TRM and the user. For this "downlink estimation", the TRM elements emit successively a known sounding signal. Each time, the user's microphone probes the CIR. Thus, instead of emitting $h_{km}(-t) * e_k(t)$, each element of the TRM now transmits $h_{mk}(-t) * e_k(t)$. As a consequence, the focusing does not depend on the channel reciprocity anymore, because the channel sounding as weel as the data transmission occur in the same direction, i.e., from the TRM to the user. However this approach has several drawbacks. First, instead of a single emission, N emissions are required to sound the channel. Of course, the more users, the less penalizing this time increase is. Indeed, the downlink and uplink estimations require K and N emissions, respectively. Second, one has to send back the channel estimations from the user to the TRM. This communication reduces the available time to transfer data.

If the second approach is used, it is important to ensure a proper synchronization of the user and sound card clocks. Indeed, having different sampling frequencies on each system would imply a bias in the computation of the channel estimation. Several experimental measurements having brought to light a difference of a few hertz between the clocks of the smartphone and the sound card, a resampling protocol has been set up.

To that end, an element of the TRM emits a 10-second-long continuous wave, of frequency equal to the central frequency of the working band. This signal allows the remote identification of the frequency with a resolution of 0.1 Hz. This estimation is used to resample the signal using a method based on a Whittaker-Shannon interpolation [AGL20].

3.3 TR Focusing

Before evaluating the communication performance in different realistic configurations, the basic focusing properties of the TRM are evaluated to assess its efficiency. To do so, the TRM time-reverses a field between 18 kHz and 19 kHz on a ME that is 1.72 meter-distant. The focal spot is recorded on two segments, centered on the ME position, with a measurement microphone mounted on a motorized linear bench; one segment is parallel (x-axis) and the other one is perpendicular (y-axis) to the TRM. The results are shown in Figure 5. The transversal and longitudinal dimensions of the focal spot can be compared to their theoretical values, given by $\lambda F/D$ and $7\lambda(F/D)^2$, respectively, where F is the focal length, D is the antenna width and λ is the wavelength. The width and length of the focal spot described by those formulas are equal to 7.2 cm and 250 cm, respectively. Because the element we focus on is shifted from the axis perpendicular to the TRM, by 16°, a simple geometrical projection implies the spot size over the x and y axs are 7.5 cm and 26 cm, respectively. These lengths are consistent with the experimental measurements. This narrow focusing effect makes this technique very sensitive to any receiver motion, because the transmission link is lost as soon as the user goes out the focal spot. Nevertheless, on the positive side, it can increase the communication security, because interception outside the focal zone is more difficult.

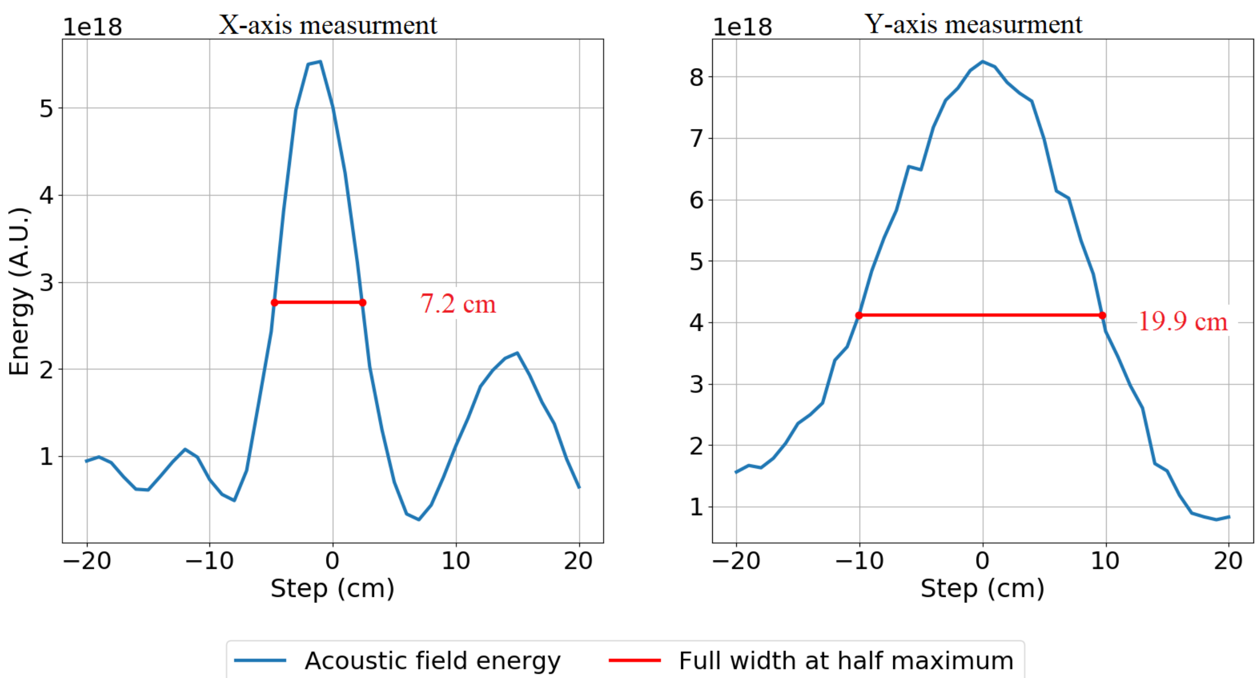

Figure 5: Focusing on a ME that is at 1.72 m from the TRM and 16° off-axis. Experimental focal spot over an axis parallel (on the left) and perpendicular (on the right) to the TRM.

4 Communications with a TRM

Here we evaluate the performance of our TR-based acoustic communication system with setup A.

4.1 Configurations

The experimental measurements were carried out in two different locations within the laboratory. First of all, we focused on Line of Sight (LoS) configurations inside a room, i.e., a configuration where there is no obstacle on the path between the transmitter and receiver. Then, the system is set up in a hallway, as well as in a small library room, for Non-Line of Sight (NLoS) configurations. Figure 6 illustrates these different configurations. For each configuration, designated by a letter, there are two "users", here MEs, identified by an index number, 1 or 2. Configuration A presents an ideal LOS case where the two MEs are facing the TRM at about 3 m and distant from each other by 1 m. Configuration B gives another example of a LOS case, but the two MEs are aligned with the axis of propagation of the TRM. In configuration C, the two MEs are close to walls (see Figure 6). Configuration D presents two NLOS cases, one in a reverberant environment (corridor) and the other one in a more attenuating environment, a library room.

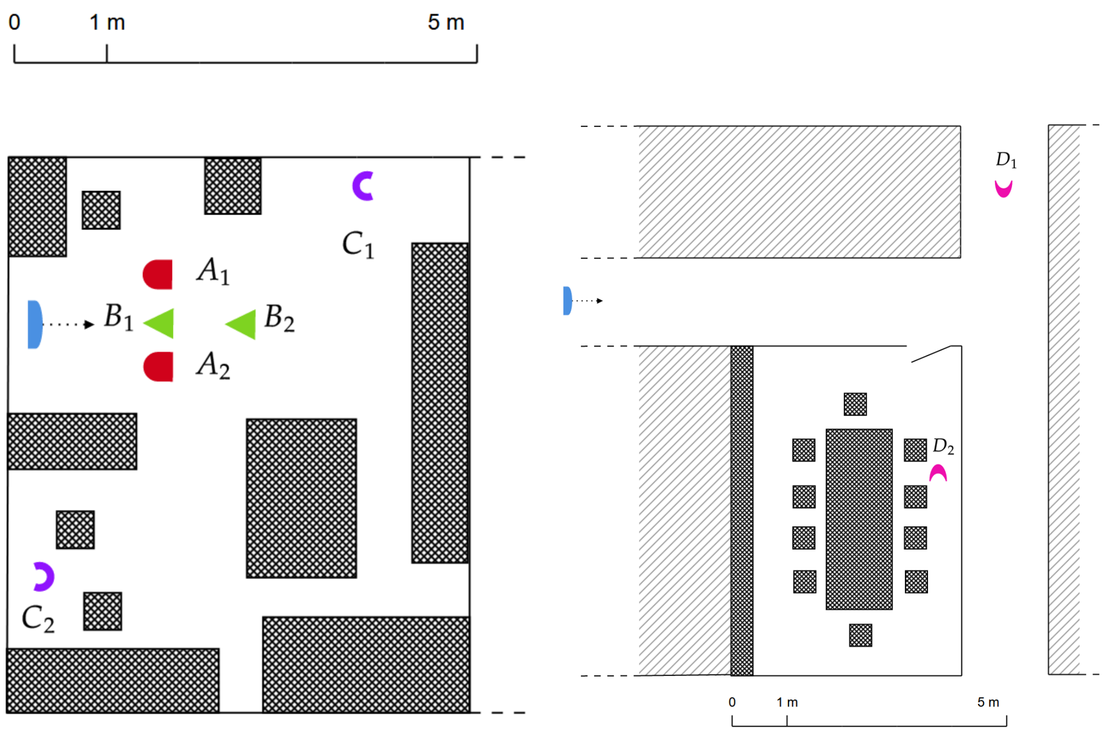

Figure 6: Left : LOS configurations in a room between a TRM (half blue ellipse) and MEs pairs (red half-ellipses, green triangles, and purple arcs). Right: NLOS configuration in a corridor and a library, between a TRM (half blue ellipse) and a MEs pair (pink crescents).

A transmitted data frame is here composed of a preamble followed five data symbols ($S_\gamma(t)$). The preamble is a 34 ms-long training rising linear chirp that is used by the receiver to detect the symbol frame and to get synchronized with it. Five chirps of duration around 17 ms encodes five bits. Depending on the bit value, the instantaneous frequency of the linear frequency chirps is either rising or falling. The preamble chirp is twice as long as a symbol chirp to increase the probability of proper detection. All chirps have a central frequency $f_c = 18.5$ kHz, and a bandwidth $B = 1$ kHz.

After focusing, the information from the data recorded on the MEs is extracted. To that end, first the received signal is correlated with the training chirp, which is known by the receiver. The value and position of the signal maximum provide a detection criterium by comparing it to a threshold level and a reference time for the frame start, respectively. Then, each received symbol is correlated with the aforementioned rising-chirp and falling-chirp. The highest correlation determines if the received chirp is considered up or down and therefore provides the value of the bit. The quality of the communication is evaluated with the computation, for each configuration, of the experimental Bit Error Rate (BER), i.e., the ratio of the number of erroneously decoded bits over the total number of transmitted bits. This statistic is estimated from the transmission of 100 frames, i.e., 500 bits. The evolution of the BER is compared to the one of the SNR. An estimation of the current noise level is obtained by computing the mean squared amplitude of the recorded signal when there is no frame transmission. As for the signal level itself, it results from the difference between the mean squared signal amplitude recorded when the training chirp is received and the noise level. Before computing these squared averaged values, the signals are filtered by a band-pass filter between 18 kHz and 19 kHz.

4.2 Communication Results

All the results of these measurements are reported in Table 1.

Configuration		A	B	C	D
ME_1	SNR (dB)	66	80	56	41
	BER (%)	0.0	0.0	0.0	0.0
ME_2	SNR (dB)	70	76	46	39
	BER (%)	0.0	11.0	0.0	0.0

Table 1: Average SNR and BER, for each ME for the 4 different configurations.

Looking first at LOS configurations, one can see that, for configurations A and C, we obtain a perfect communication quality, i.e., without errors during decoding. As expected, when moving away from the TRM, the SNR decreases of 10 dB and 24 dB, respectively for ME_1 and ME_2, compared to configuration A. For the case of configuration B, while the SNR ratio is very good, a significant BER is observed on the ME #2. Indeed, the focal spots of the 2 MEs overlap and induce strong IUI.

Regarding the NLOS configuration, we can see that the TRM also allows perfect communications to be carried out. As expected in the absence of a direct path, we note a significant decrease in SNR of 25 dB and 31 dB, respectively for ME_1 and ME_2, compared to configuration A.

Those results can be interestingly compared to the case of a conventional transmission scheme with a single emitting element for configurations A and C. The comparison looks at the relative SNR between these schemes when the same power is used for the emission, whichever the transmission scheme. The results are shown in Figure 4.2. Compared to the case of a single emitter, the TRM brings a significant SNR gain of 24 dB and 27 dB when focusing on a single user and of 14 dB and 23 dB when focusing on two users. As expected, the SNR is higher when the focusing is achieved on one single point rather than two. It can also be noted that, by moving away from the TRM (configuration C), the difference between these two patterns decreases significantly.

5 Communication with a Smartphone

We evaluate in this section our communication system between the TRM and a more realistic receiving device, a smartphone (setup B). The communication has also been tested in different environments.

5.1 Experimental Setup

We use, in this section and the next, a fairly recent (about a year old) and mid-range smartphone: an Honor Play. It has a loudspeaker and a voice microphone (VM), spaced approximately by mm, on its lower edge, and a "surround" or ambient microphone (AM) on its upper edge. The two microphones have the

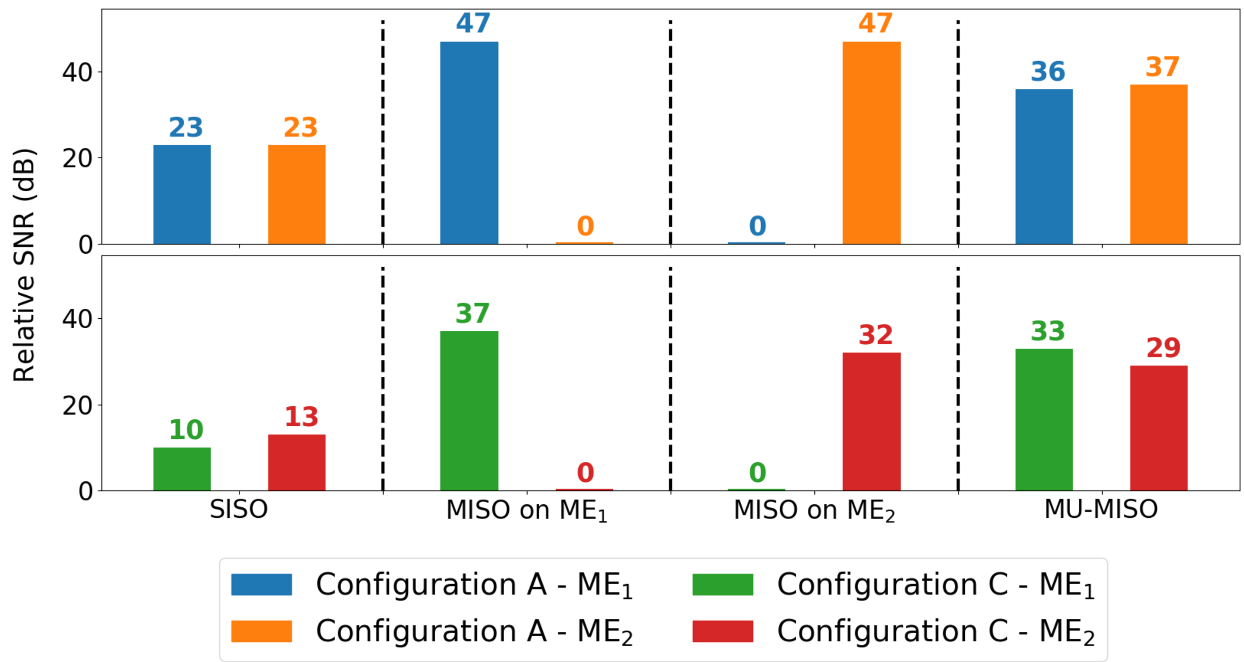

Figure 7: Relative SNRs - obtained with a single emitter, a TRM focusing successively or simultaneously on two users - for configurations A and C. The transmission power is held constant.

same characteristics and are not co-located with the speaker. The sending of instructions and the recovery of signals between the laptop and the smartphone are managed by a dedicated application using a Wi-Fi connection, developed as part of this research work.

As for the MEs before, the smartphone was acoustically characterized in the anechoic chamber at Sorbonne University. We found characteristics similar to the ME's in terms of opening angle at -3 dB, with about 55 degrees in transmission and 30 degrees in reception. However, by studying the frequency responses for the elements of the ME and the smartphone, one can see that those are less stable in the case of the smartphone. This may presage lower performance than the ME.

5.2 Experimental Protocol

The time-reversal process begins here again with a learning step to estimate the propagation channel. However, the complexity of this step increases here, since we have to consider two distinct channels, i.e., TRM/VM and TRM/AM, and two methods for estimating the propagation channel. Focusing via downlink channel estimation (DCE) will allow focusing on each microphone, while focusing via uplink channel estimation (UCE) will highlight the effects of the non-co-localization of the loudspeaker and microphones.

As before, the experimental measurements were carried out in three different places within Institut Langevin, thus making it possible to test LOS and NLOS configurations. Figure 8 illustrates these different configurations. Configuration E presents an ideal LOS case where the smartphone is facing the TRM, at about 3 m, arranged parallel to the axis of propagation. The variant E* uses this configuration, but this time with a phone arrangement perpendicular to the axis of propagation. Configuration F concerns the case where the smartphone is close to the walls of the rooms and outside the opening angle of the TRM. Configuration G presents the NLOS case in a mixed environment (library).

The experimental measurements were also carried out in a basement, at the MINES ParisTech school in Paris, which is a more difficult environment (see Figure 9). Configuration H presents a LOS case where the smartphone is 22 m from the TRM. This distance increases to about 40 m for configuration I, representing a LOS case. The configuration J is an NLOS configuration where the smartphone and the TRM are 15 m apart, with a bend of 8 m.

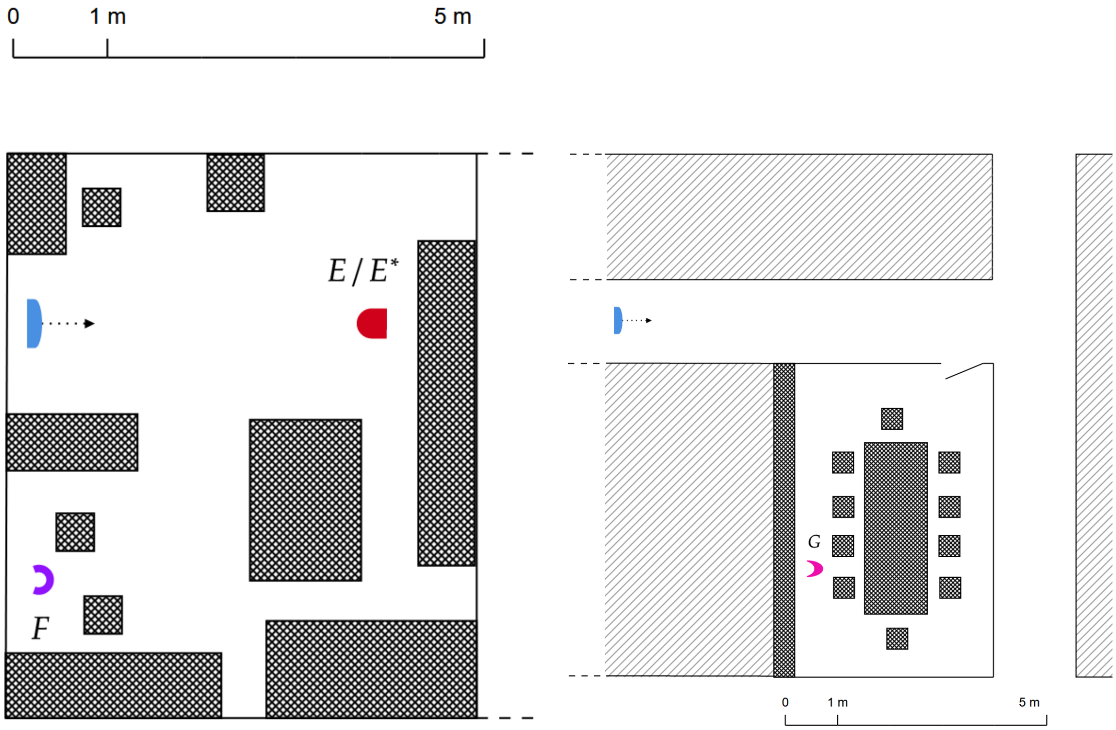

Figure 8: Left: LOS configurations in a closed rooms between a TRM (blue half ellipse) and a smartphone (red half-ellipse and purple arc). Right: NLOS configuration in a corridor and a library between a TRM (blue half ellipse) and a smartphone (pink crescent).

5.3 Symbol Focusing

The symbol-focusing measurements are carried out by focusing a rising chirp with central frequency $f_c = 18.5$ kHz, bandwidth $B = 1$ kHz and symbol time $T = 768$ samples (~ 17 ms), at a sampling frequency $f_e = 44.1$ kHz. For each transmission of the symbol, the recorded signal is successively correlated with the rising and falling chirps. The result of the two correlations are noted $C_{\nearrow}(t)$ and $C_{\searrow}(t)$, respectively. The figure 10 gives an example of such correlations..

From these two correlations, we introduce the "decoding contrast" η as the ratio of the maxima of the envelopes of $C_{\nearrow}(t)$ and $C_{\searrow}(t)$. The larger this ratio is, the more robust to noise the transmission is, because the easier the receiver can distinguish the symbols from each other. The values of η, for all the configurations, are gathered in Table 2. In the same table is also shown the relative maximum value C_{max} of the correlation $C_{\nearrow}(t)$.

We note that for almost all the configurations, DCE makes it possible to obtain very good contrasts and thus suggests a good quality of communication. Only the contrast of configuration J is weak, probably due to a noisy environment. Indeed, the AM was there directed toward a noisy central heating system. As regards the uplink estimation, we see that the contrast also gives decently good results for the LOS configurations on the VM. However, in the case of NLOS configuration, the focal spot on the loudspeaker could be as small as half-a-wavelength, i.e., 1cm, [DF97], which is here smaller than the distance between the VM and the loudspeaker. As a result, the quality of the reception by the VM is very low. In addition, this effect occurs in both LOS and NLOS configurations for the AM, because this microphone it is more than 15 cm away from

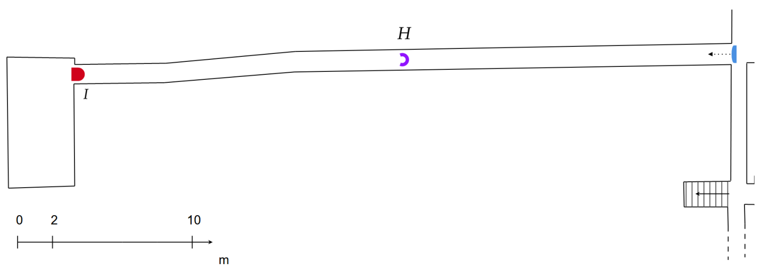

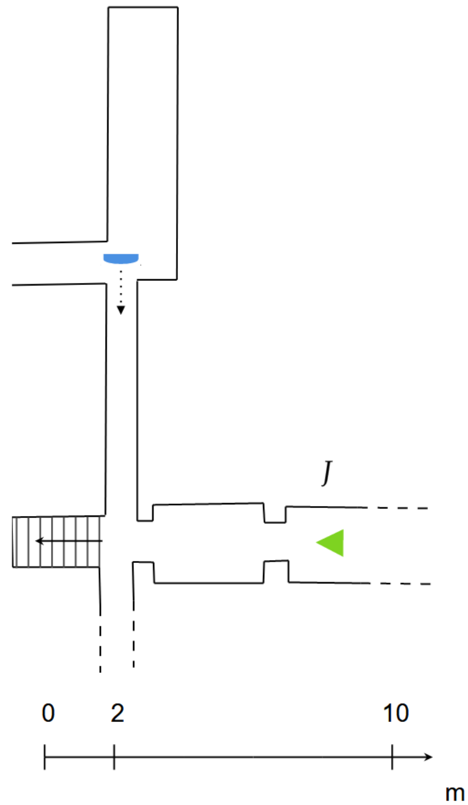

Figure 9: Left: LOS configurations in a basement between a TRM (half blue ellipse) and a smartphone (red half-ellipse and purple arc). Right: NLOS configuration in a basement between a TRM (half blue ellipse) and a smartphone (green triangle).

the loudspeaker.

In general, the maximum values of the correlation are larger in LOS than in NLOS. It is only not the case in the basement, because even if configuration I is in LOS, the smartphone is 25 m farther from the TRM as in the case of NLOS configuration J.

5.4 Communication Results

The communication measurements are carried out with the same protocol as the one described in Section 4.1. But because it takes more time to transfer a frame between the smartphone and the computer via the application, the BER is estimated from the acquisition of 100 bits (transmission of 20 frames) instead of 500 bits. The results are reported in Table 3.

In the laboratory, as we expected, the DCE provides excellent results whichever the configuration. For the uplink case, the transmission quality is very poor. Note that in general the BER obtained on the AM is close to 50%, that is to say the decoded bits are almost completely random. As observed in the previous section, this is because the AM is outside the focal spot. The BER is lower for the VM, because this last one is much closer to the loudspeaker and, therefore, the signal is a little bit less distorted. However, for configuration E, the BERs acquired on AM and VM are similar. Even if this equivalent behavior does not clearly appear on the contrast scale (see Table 2), in this LOS configuration, the AM and VM are probably inside the same elongated focal spot.

In the basement, the results are worse. Contrarily to what the symbol focusing results could have suggested, we notice that DCE only allows a very good quality of communication, with a BER of 0%, on the VM

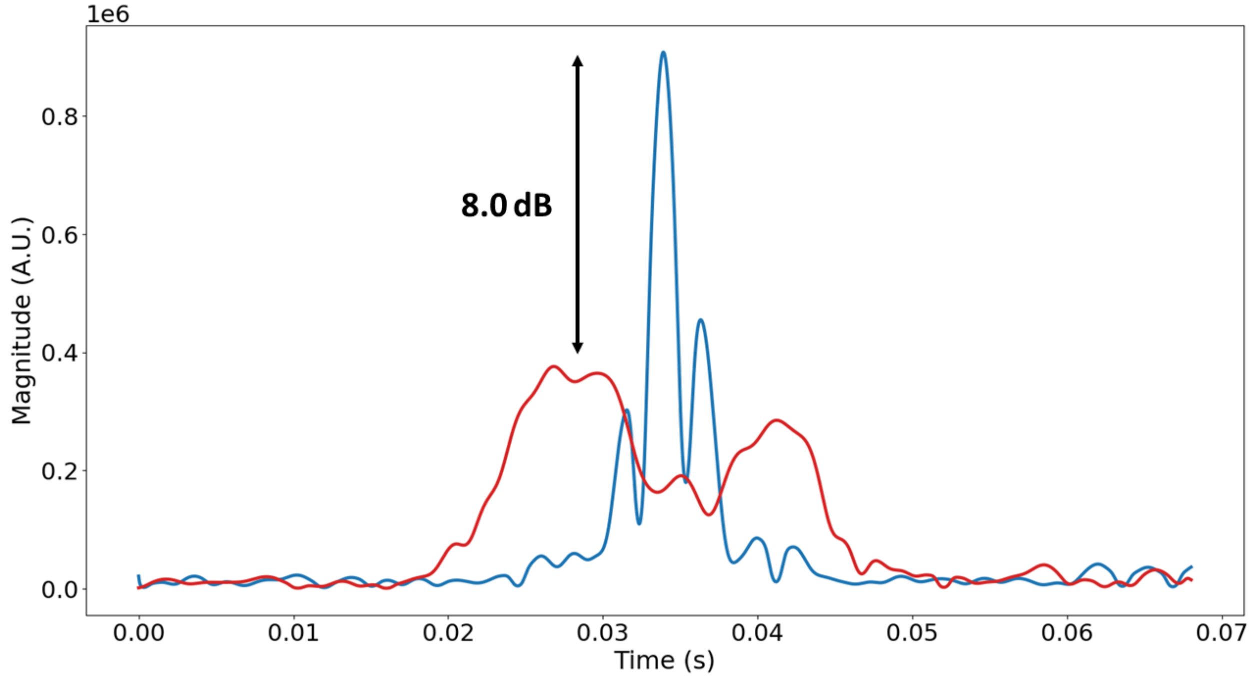

Figure 10: Envelopes of $C_{\nearrow}(t)$ (blue curve) and $C_{\searrow}(t)$ (red curve) for a symbol transmission between the TRM and the VM in the case of configuration E. The symbol is focused using the UCE.

for the H and I configurations. For configuration J, the BER increase is probably due to the proximity of a noisy central heating and a NLOS configuration. The error rate is large for the AM whichever the channel acquisition method and configuration. Actually, for all the configurations, the smartphone and the corridor axis were aligned, the AM being oriented in a direction away from the TRM. As a consequence of the microphone directivity pattern and the waveguide geometry of the corridor, which prevents sound backscattering, as it can be seen in Table 2, the TRM generates a weak signal level on the AM that is therefore very sensitive to noise. As for the UCE, the BER is high because of the conjugate effect of the non-co-localization of the microphones and loudspeaker and the weak energy level.

6 Discussion

The various experimental results obtained previously make it possible to globally evaluate the communications carried out with a TRM in a near-ultrasonic range with ideal transceivers or a non-dedicated device in actual environments. The first highlight is the gain brought by the use of a TRM compared to conventional communication techniques, i.e., with a base made of a single emitter. Because of the ensuing increase of SNR, error-free communications has been obtained even in NLOS configurations. Because a TRM can take advantage of the spatial diversity, it is able to focus two different messages simultaneously to two users as long as the focal spots associated with one user does not overlap with the one of the other user.

However, with a non-dedicated device as a user, due to the frequent non-co-localization of the speaker and microphones, the simplest and fastest channel acquisition technique, i.e., the uplink one, provides poor transmission results. However, at the cost of a more complex procedure that requires to send back to the TRM the channel estimations, our results suggest that it is possible to maintain a very good quality of communication, without errors.

Finally, it appears that, in a constrained environment where strong energy losses occur, the focusing effect is not sufficient to compensate the signal attenuation, especially for microphones that are oriented in opposite

	DCE				UCE			
	VM		AM		VM		AM	
	η	C_{max}	η	C_{max}	η	C_{max}	η	C_{max}
E	8	0	6	-7	8	0	3	-6
E*	7	-3	7	-7	5	-2	3	-1
F	8	-10	8	-13	5	-5	-1	-6
G	7	-13	9	-16	2	-12	0	-13
H	7	0	5	-5	6	0	2	-5
I	8	-12	8	-14	0	-7	1	-12
J	7	-4	2	-5	1	-1	0	-9

Table 2: Values of η and C_{max} , in dB, for VM and AM, with DCE and UCE, for all the configurations. C_{max} values for E, E*, F, G (respect., H, I, J) are normalized with respect to the maximum value obtained for configuration E (respect., H).

	Ch. est.	DCE		UCE	
	Microphone	VM	AM	VM	AM
Config.	E	0	0	26	27
	E*	0	0	22	41
	F	0	0	27	51
	G	0	0	22	43
	H	0	25	0	37
	I	0	30	40	46
	J	10	40	43	38

Table 3: Value of BER, in percentage, for VM and AM, with DCE and UCE, for all the configurations.

direction to the TRM.

From these observations, we may consider viable the use of a communication system similar as the one introduced in this paper in specific situations such as:

- high-speed data transfer on short-distance LOS configurations according to a MIMO transmission scheme, by segmenting information and focusing it simultaneously at several points in space;
- bidirectional communication with an isolated operator in a constrained environment, in LOS and NLOS configurations, e.g., undergrounds, hangars or ATEX zones;
- communication with a limited number of transmitters that, nonetheless, need to cover a large area, e.g., an amphitheater or a train station, using either a large transmission aperture or a scanning method.

7 Conclusion

In this paper, we have presented the first use of a time-reversal mirror (TRM) for indoor communications with near ultrasound, in actual and constrained environment. We have shown its advantages over existing techniques, regarding the SNR, BER and ability to manage obstacles and NLOS situations. Perfect communication with BERs of 0% have been obtained in indoor configurations with dedicated transceivers. We have observed and quantified the impact of the non co-localization of microphones and speaker, which, in the case of a smartphone, strongly increases the BER in the case of UCE. The experimental - results of this research work allow us to identify venues for future work. First of all, one could think about optimizing the ME and the associated audio processing blocks (amplification and pre-amplification). Then, it would be interesting to study other geometries of antenna, and in particular sparse antennas. It would also be exciting to consider a MIMO transmission scheme between two TRMs.

References

[CWF90] Didier Cassereau, François Wu, and Mathias Fink. “Limits of self-focusing using closed cavities and mirrors - Theory and experiments”. In: hawaii, 1990, pp. 1613–1618.

[PWF91] Claire Prada, Feng Wu, and Mathias Fink. “The iterative time reversal mirror: A solution to self-focusing in the pulse echo mode”. In: *Journal of Acoustical Society of America* 90.2 (1991).

[CF92] Didier Cassereau and Mathias Fink. “Time-reversal of ultrasonic fields. III. theory of the clo- sed time-reversal cavity”. In: *IEEE Transactions on ultrasonics, ferroelectrics, and frequency control* 39.5 (1992), pp. 579–592.

[Fin92] Mathias Fink. “Time Reversal of Ultrasonic Fields - Part I : Basic Principles”. In: *IEEE Transactions on ultrasonics, ferroelectrics, and frequency control* 39.5 (1992).

[FWT92] Mathias Fink, François Wu, and Jean-Louis Thomas. “Time Reversal of Ultrasonic fields. Part II. Experimental results”. In: *IEEE Transactions on ultrasonics, ferroelectrics, and frequency control* 39.5 (1992), pp. 555–566.

[CFW95] N. Chakroun, M.A. Fink, and F. Wu. “Time reversal processing in ultrasonic nondestructive testing”. In: *IEEE Transactions on Ultrasonics, Ferroelectrics, and Frequency Control* 42 (6 1995), pp. 1087–1098. ISSN: 1525-8955. DOI: `10.1109/58.476552`.

[DRF95] Arnaud Derode, Philippe Roux, and Mathias Fink. “Robust Acoustic Time Reversal with High-Order Multiple Scattering”. In: *Physical Review Letters* 75.23 (Dec. 1995), pp. 4206–4209. DOI: `10.1103/PhysRevLett.75.4206`. URL: `https://ui.adsabs.harvard.edu/abs/1995PhRvL..75.4206D`.

[TF96] J-L Thomas and Mathias A Fink. “Ultrasonic beam focusing through tissue inhomogeneities with a time reversal mirror: application to transskull therapy”. In: *IEEE transactions on ultrasonics, ferroelectrics, and frequency control* 43.6 (1996), pp. 1122–1129.

[TWF96] Jean-Louis Thomas, François Wu, and Mathias Fink. “Time reversal focusing applied to lithotripsy”. In: *Ultrasonic imaging* 18.2 (1996), pp. 106–121.

[DF97] Carsten Draeger and Mathias Fink. “One-Channel Time Reversal of Elastic Waves in a Chaotic 2D-Silicon Cavity”. In: *Physical Review Letters* 79.3 (July 1997), pp. 407–410. DOI: `10.1103/PhysRevLett.79.407`. URL: `https://ui.adsabs.harvard.edu/abs/1997PhRvL..79..407D`.

[Fin97] Mathias Fink. “Time Reversed Acoustics”. In: *Physics Today* 50.3 (1997), pp. 34–40.

[Ede+02] G.F. Edelmann et al. “An initial demonstration of underwater acoustic communication using time reversal”. In: *Oceanic Engineering, IEEE Journal of* 27.3 (2002), pp. 602–609. URL: `http://ieeexplore.ieee.org/xpls/abs_all.jsp?arnumber=1040942`.

[Der+03] Arnaud Derode et al. “Taking advantage of multiple scattering to communicate with time-reversal antennas”. In: *Physical Review Letters* 90.1 (2003), p. 014301.

[YTF03] Sylvain Yon, Mickael Tanter, and Mathias Fink. “Sound focusing in rooms: the time-reversal approach”. In: *The Journal of the Acoustical Society of America* 113.15533 (2003).

[Can+04] James V. Candy et al. “Time-reversal processing for an acoustic communications experiment in a highly reverberant environment”. In: *The Journal of the Acoustical Society of America* 115 (2004), p. 1621.

[Ler+04] G. Lerosey et al. “Time Reversal of Electromagnetic Waves”. In: *Phys. Rev. Lett.* 92 (19 May 2004), p. 193904. DOI: `10.1103/PhysRevLett.92.193904`. URL: `https://link.aps.org/doi/10.1103/PhysRevLett.92.193904`.

[SKC04] K. Sarabandi, I. Koh, and MD Casciato. "Demonstration of time reversal methods in a multi-path environment". In: *Antennas and Propagation Society International Symposium, 2004. IEEE.* Vol. 4. IEEE. 2004, pp. 4436–4439. URL: http://ieeexplore.ieee.org/xpls/abs_all.jsp?arnumber=1330336.

[WRC04] Chun H Wang, James T Rose, and Fu-Kuo Chang. "A synthetic time-reversal imaging method for structural health monitoring". In: *Smart materials and structures* 13.2 (2004), p. 415.

[Can+05] James V. Candy et al. "Multichannel time-reversal processing for acoustic communications in a highly reverberant environment". In: *The Journal of the Acoustical Society of America* 118 (2005), p. 2339.

[Ler+05] G Lerosey et al. "Time reversal of electromagnetic waves and telecommunication". In: *Radio science* 40.6 (2005).

[ZGQ06] C. Zhou, N. Guo, and R.C. Qiu. "Experimental results on multiple-input single-output (MISO) time reversal for UWB systems in an office environment". In: *Military Communications Conference, 2006. MILCOM 2006. IEEE.* IEEE. 2006, pp. 1–6. URL: http://ieeexplore.ieee.org/xpls/abs_all.jsp?arnumber=4086874.

[El-+10] H. El-Sallabi et al. "Experimental Investigation on Time Reversal Precoding for Space–Time Focusing in Wireless Communications". In: *Instrumentation and Measurement, IEEE Transactions on* 59.6 (2010), pp. 1537–1543. URL: http://ieeexplore.ieee.org/xpls/abs_all.jsp?arnumber=5457979.

[AB11] Will Archer Arentz and Udana Bandara. "Near ultrasonic directional data transfer for modern smartphones". In: Association for Computing Machinery, 2011, pp. 481–482. ISBN: 978-1-4503-0630-0. DOI: 10.1145/2030112.2030181. URL: https://doi.org/10.1145/2030112.2030181.

[LR12] Patrick Lazik and Anthony Rowe. "Indoor Pseudo-ranging of Mobile Devices using Ultrasonic Chirps". In: *SenSys'12* (2012).

[Dub+13] Thierry Dubois et al. "Performance of time reversal precoding technique for MISO-OFDM systems". In: *EURASIP Journal on wireless communications and networking* 2013.1 (2013), p. 260.

[Dub+14] T. Dubois et al. "Efficient MISO system combining Time Reversal and OFDM/OQAM". In: *Proc. European Wireless 2014; 20th European Wireless Conf.* May 2014, pp. 1–5.

[Kon+15] Chuili Kong et al. "Sum-rate and power scaling of massive MIMO systems with channel aging". In: *IEEE Transactions on Communications* 63.12 (2015), pp. 4879–4893.

[VTS15] Carlos A Viteri-Mera, Fernando L Teixeira, and Kamalesh Sainath. "Interference-nulling time-reversal beamforming for mm-Wave massive MIMO systems". In: *Microwaves, Communications, Antennas and Electronic Systems (COMCAS), 2015 IEEE International Conference on.* IEEE. 2015, pp. 1–5.

[Wan15] Quan Wang. "Non-linear chirp spread spectrum communication systems of binary orthogonal keying mode". PhD thesis. 2015.

[BLM16] E. Björnson, E. G. Larsson, and T. L. Marzetta. "Massive MIMO: ten myths and one critical question". In: *IEEE Communications Magazine* 54.2 (Feb. 2016), pp. 114–123. ISSN: 0163-6804. DOI: 10.1109/MCOM.2016.7402270.

[JW16] Wentao Jiang and William M. D. Wright. "Full-Duplex Airborne Ultrasonic Data Communication Using a Pilot-Aided QAM-OFDM Modulation Scheme". In: *IEEE Transactions on ultrasonics, ferroelectrics, and frequency control* (2016).

[Son16] Hee-Chun Song. “An overview of underwater time-reversal communication”. In: *IEEE Journal of Oceanic Engineering* 41.3 (2016), pp. 644–655.

[Get+18] Pascal Getreuer et al. “Ultrasonic Communication Using Consumer Hardware”. In: *IEEE Transactions on Multimedia* 20.6 (2018), pp. 1277–1290.

[AGL20] Almudena Antuña, Juan Guiraro, and Miguek López. “Shannon-Whittaker-Kotel’nikov’s theorem generalized revisited”. In: *Journal of Mathematical Chemistry* 58 (2020).